SCIREA Journal of Materials Science

http://www.scirea.org/journal/Materials

November 11, 2016

Volume 1, Issue1, October 2016

Structural Quality Promotion of Vanadium-Containing Biotite via Gamma Irradiations

Khaled M. Elsabawy[1,2,*] and Ahmed T.Tawfik[1,3]

[1]Materials Science Unit ,Chemistry Department ,Faculty of Science, Tanta University - 31725-Tanta-Egypt

[2] Faculty of Science-Chemistry Department-Taif University-Taif–Alhawyah -888-Saudia Arabia

[3] Egyptian Environmental Affairs Agency-Egypt

ABSTRACT

Advanced synthesis of free fluoride V-biotite sample having the optimized formula $NaV_{2.5}(Al,Si)_4O_{10}(OH)_2$ was synthesized by mixed solution-solid routes. The synthetic clay was carefully characterized by different techniques including X-ray diffraction (XRD), infrared absorption spectra (IR) and thermal analysis (TG/TDA).Furthermore micro-structural features were monitored by both of scanning electron microscopy (SEM) and AFM . The synthetic clay sample was exposed to two different gamma irradiation doses ,1st dose was 2 MR and 2nd dose ~ 4MR. Structural measurements after γ-irradiations gave structure quality for synthetic V-biotite clay due to disappearance of some impurity phases and unreacted oxides as result of absorbed gamma-ray dose increases from 2 to 4 MR .

Keywords: Biotite, Clay, XRD, TGA, SEM,AFM, Green synthesis.

I. Introduction

Gamma, Laser irradiations doses were applied as structure promoters for different kinds of matters such as glass, ceramics and mineral clays[1-3]. Rare earth doped phosphors have a vital role as radiation detectors in many fields of fundamental and applied research, such as clinical, personal, and environmental monitoring of ionizing radiation [4,5]. Various methods of preparation have also been developed for easy synthesis of these materials to make them available easily. While irradiation usually leads to the creation of structural defects, the healing effect of irradiation is also known [6-7]. Ionizing radiation has been found to be widely applicable in modifying the structure and properties of polymers and can be used to tailor the performance of either bulk materials or surfaces. Improved luminescent characteristics of some of aluminates have also found their place in optoelectronics. The thermo-luminescence (TL) materials have been widely applied to defect studying and dosimetry, such as the detection of ionizing radiation and dating in archaeology [8-13]. The ability to detect and perform energy-dispersive spectroscopy of high-energy radiation such as X-rays, γ-rays, and other uncharged and charged particles has improved dramatically in recent years [14]. Alkaline earth aluminate ceramics are important host materials that have been prepared and studied by several researchers for luminescence applications [15]. Alkaline earth aluminate belongs to the spinel group of minerals (MAl_2O_4) with general chemical composition, AB_2O_4, where A is a divalent atom [16]. The magnesium aluminate spinel ($MgAl_2O_4$) has good thermal and mechanical properties, high hardness and low electrical loss, and chemical properties. As such, it is currently utilized as a refractory for furnace walls and firebricks and also has the potential for application as environment humidity sensors, laser materials, and substrate in integrated electronics [17-21].

The major goal of these investigations is proving that irradiations doses can promote and enhance structure of solid materials towards more regular structure eliminating defects could be caused by impurity phases.

II. Experimental

II.1. Materials

All reagents used were of analytical grade (each purity >99%) Al_2SiO_5 from BHD Laboratory reagent, Na_2CO_3 (GPR), and ammonium meta-vanadate, NH_4VO_3 (A.R. grade for laboratory

and research uses) were mixed in the chemical compositions corresponding to synthesizing $\{NaV_{2.5}(Al,Si)_4O_{10}(OH)_2\}$which have chemical formula of V-biotite.

II.2. Synthesis of V-Biotite Clay Sample

V-biotite was prepared carefully by using mixed solution/solid- state reaction technique using nominal compositions of individual oxides in the main formula, such that aluminum silicate $Al_2O_3.SiO_2$, sodium carbonate (anhydrous) Na_2CO_3 were dissolved 50 ml of concentrated solution of HNO_3 then diluted to 100 ml by distill H_2O solution (I). Ammonium meta-vanadate NH_4VO_3 is also dissolved in the same amount of nitric acid with same dilution factor , solution(2). The obtained solution (I+II) were mixed together and coprecipitated by conc. ammonia/citrate solution, the hydroxylated precipitated product was filtered and dried in oven at 110 ℃.

The powders mixtures were mixed in an agate mortar for 1 h. The green compacted metals powder was subjected to firing in a controlled atmosphere furnace to a temperature below its melting point in sealed platinum container at 900-950 ℃ for 9 h, followed by sintering step at 880 ℃ to allow packed metal powders to bond together and finally, the furnace was cooled slowly down to room temperature and the material was kept in vacuum desiccators over silica gel dryer.

II.3. Characterization of V-Biotite Clay Sample

II.3.1 X-ray diffraction investigation

XRD powder diffraction measurements were performed on an X'Pert SW. X-ray diffractometer with filtered Cu Kα radiation (λ=1.54 A°), at 40 Kv and 30mA with a scanning speed in the range of 2θ=5-70 (298 K)**.**

II.3.2 Infrared spectra studies

The IR spectra of the clays were recorded between 4000 and 400 cm^{-1} using a KBr method with a NICOLET 6700 FTIR thermoscientific spectrophotometer.

II.3.3. SEM and AFM Investigations

Scanning electron microscope measurement was carried out using small pieces of the prepared sample by using a “Philips model XL 30 CP”. The sample was coated with gold. Scanning electron microscope (SEM) was used to take micrographs of the clays. AFM investigations made by di-innova (USA) instrument accompanied with particle size analyzer,

tapping non-contact mode was applied on small piece of the prepared clay after gamma irradiations .

II.3.4. Thermal studies

Thermogravimetry (TGA) and differential thermal analysis (DTA) were carried out by using a Shimadzu DTA-50H thermal analyzer. The sample was placed in platinum crucible (0.1 cm^3) the system were studied under nitrogen atmosphere with a heating rate 10 ℃ min^{-1} and following rate at 20 ml min^{-1} , constant weight of sample 4.7 mg was used.

II.3.5. Electrical conductivity studies

The DC-electrical conductivity of synthetic V-biotite was measured using two terminals DC-method. The pellets were inserted between spring loaded copper electrodes, A KEITHLEY 175 multimeter (ASA) was employed from 10-500 ℃.

The temperature was measured by a calibrated chromel-alumel thermocouple placed firmly at the sample. Measurements were conducted in such a way that at each temperature, sufficient time was allowed to attain thermal equilibrium.

The number of conduction electron n is given by:

$n = n_o e^{-Eg/KT}$ ……………………………………(2)

where n_o **is** the concentration of atoms at the lattice site, E_g is the band gap, and K is the Boltezman constant (assuming $E_g \approx KT$), the conductivity relationship becomes

$\sigma = (n_o e^{-Eg/KT}) e\mu$ ……………………………………(3)

$\sigma = Ae^{-Eg/KT}$ where $A= n_o e\mu$ ………………..(4)

$\text{Log } \sigma = \text{Log } A-(E_g/2.303KT)$ ……………………..(5)

The plot of log σ against 1/T should give a straight line with a slop of –E/2.303K.

The measurements of σ as a function of temperature will permit calculation of the band gap energy E_g of materials behavior (conductor, semiconductor and insulator)

III. Results and Discussion

Fig.(1a-c): shows the XRD pattern recorded for synthetic free fluoride biotite which has the formula $NaV_{2.5}(Al,Si)_4O_{10}(OH)_2$

Fig.1a is for non-irradiated V-biotite sample while Fig.1b and Fig.1c are for gamma-irradiated V-biotite with absorbed γ-dose ~2 MR and 4 MR respectively .The XRD analysis of corresponding 2θ values and interplanar spacing d(Å) were carried out using a computerized program(Gesas), a change in the interlayer distance than the original phyllosilicates is observed because replacement of potassium ions with sodium ions and without using fluorine in the structure formation. The d(001)-spacing of natural micas with potassium ions in their interlayer is ≈ 10 Å [16] .one indicate that after gamma irradiations the monoclinic phase of biotite clay is promoted by degree ~ 3-4 % in contrast with non-irradiated sample of mica-clay .The dominating monoclinic phase exceeds than 95% confirming that nano-oxide component are successfully reacted through mixed solution/solid techniques and formed monoclinic biotite phase with very good degree of crystallinity[17].

The FTIR spectra of V-biotite have shown in (Fig. 2a-c) it is clear that gamma irradiation doses has narrow and very limited effects on the peak positions of the functionalized groups that present on the V-biotite clay .As it clear in Figs.2a-c the bands in the 4000-2000 cm^{-1} rang corresponding to the vibrations of the V-OH group and coordinated water. Bands in the 1200-600 cm^{-1} rang characteristic of silicate; band centered at 1030 cm^{-1} was attributed to Si-O-Si asymmetric stretching mode. The peak at 621 cm^{-1} was assigned to O-Si-O asymmetric stretching as reported in silicate system [18].

Fig. 3 represents the (TGA–DTA) curves of non-irradiated green mixtures of V-biotite. From this figure it can be seen that: (i) The TGA-curve of this sample consisted of three weight loss processes in temperature ranged between (173)–(215) ◦C, (425-556) ◦C and (856)–(994.) ◦C. The first two steps represented the thermal decomposition of ammonium metavanadate into different types of vanadyl compounds species as, $(NH_4)_2V_6O_{16}$ and $NH_4V_4O_{10}$ with a constant weight losses of 2.9% and 0.44%, before the formation of V_2O_5 as a final product with a constant weight loss of 2.2% at 994 ◦C. (ii) The DTA-curve of this solid consisted of three endothermic peaks their minima located at 98, 190 and 400 ◦C. In addition, strong and broad exothermic peak; its maxima; located at 850 ◦C was detected without the observation of any weight change in the TG-curve. This peak might correspond to the formation of solid state reaction [19, 20]

Scanning electron micrographs (SEM) image indicates the morphology and grain size of the mica particles before and after gamma-radiation. The sample v-biotite has a flake-like morphology, which is typical for this synthetic mica (Figs.4a-c). However, the particles appear to have aggregated, which would influence the surface area [21-22]. The estimated

average grain size was found in the range of 2-4 μm with a particle sizes 0.5μm, which influence the surface area. This type of morphology is typical for synthetic clays and supporting the data reported [23].

While the estimated crystallite size of detected phase was calculated using Scherrer's equation and found to be 55 nm. This indicates that, the actual grain size in the material bulk is smaller than that detected on the surface morphology of investigated clay. This trend of grain size error detection was observed by many authors as [24,25].

Fig.5 displays 2 and 3D-AFM imaging for non-irradiated v-biotite mica it was observed that the grain size in the surface is nearly equal to that reported by SEM investigations ~ 2-4 μm.

These results confirmed that applied advanced technique is yielding homogeneous product by additional to gamma-irradiations make as collector to the smaller graing in material bulk to give unified grain size average lies in between 2-5μm.

The temperature dependence of the electrical conductivity of synthetic V-biotite shows in (Fig. 6). The electrical conductivity at a given temperature is significantly lower after heating than before heating. We conducted stepwise heating experiments of biotite. With increasing the temperature the conductivity decreases and gradually reaches a stationary value. Then the conductivity increase at a fixed temperature is not significant below 450 ℃. Remarkable increase is observed at the temperature of 450-500 ℃. The conductivity increase is not significant above 500 ℃. The band gap energy result calculated from fig.6 was 359 JK^{-1} this mean that the synthetic V-biotite has insulator behavior. The result can be interpreted as the resistivity of a metal arises from the scattering of the conduction electron by static lattice defects such as vacancies and thermal scatters which are created by the thermal motion of atoms or electrons [26].

IV. Conclusions

The conclusive remarks inside this work could be summarized as follows:

1- Green synthesis of free-fluoride V-biotite is valid .

2- SE-micrographs analysis confirmed that free fluoride $NaV_{2.5}(Al,Si)_4O_{10}$ $(OH)_2$ has meso-porous structure with grain size in the range between 2-4 μm and a particle size average 0.5μm, while from Scherrer's calculations found to be 55 nm confirming the actual grain size

in the material bulk is smaller than that detected on the surface morphology of investigated clay.

3- Gamma-irradiations make as structure promoter as proved in our XRD and SEM investigations.

4- AFM-investigations confirmed SEM which is reflecting structure homogeneity and success of synthesizing technique.

Figures and Tables

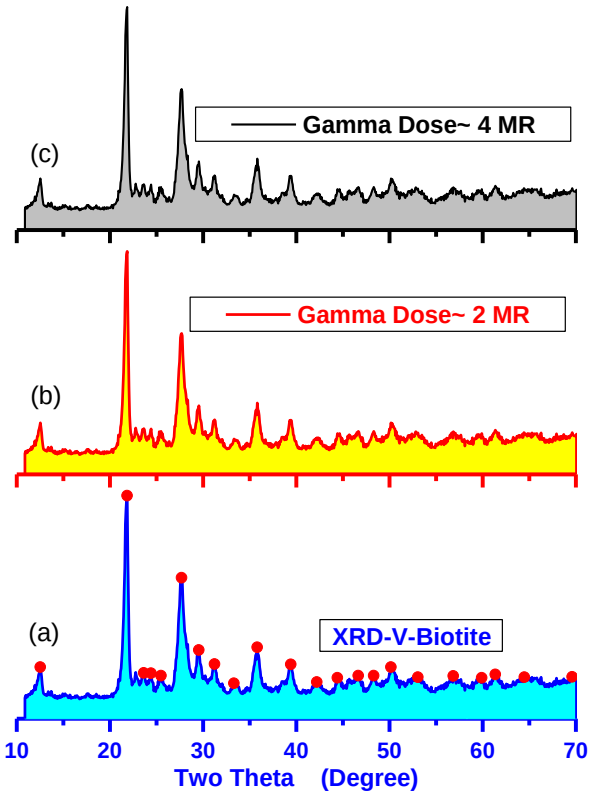

Fig. 1a-c: XRD patterns recorded for V-biotite before and after gamma irradiations.

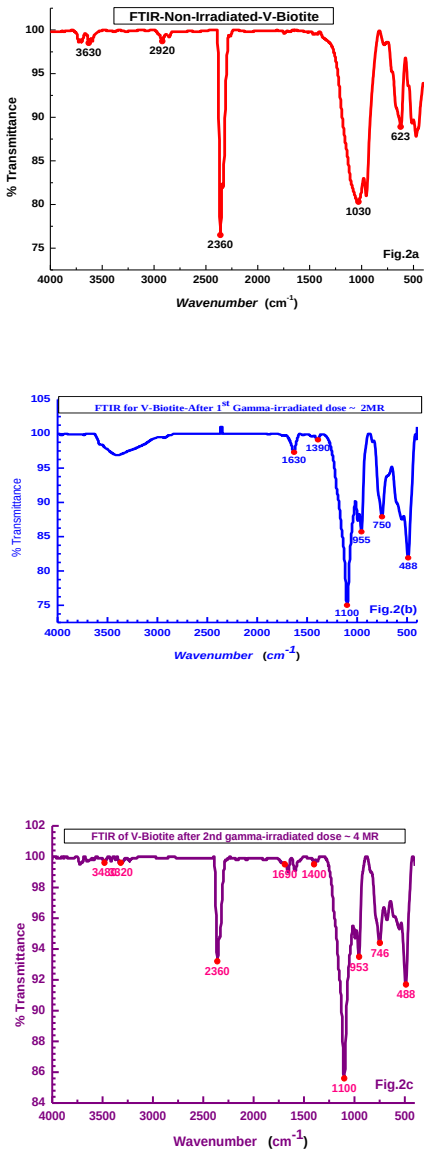

Fig.2a-c: FTIR-spectra recorded for V-biotite sample before and after two different doses of gamma ray .

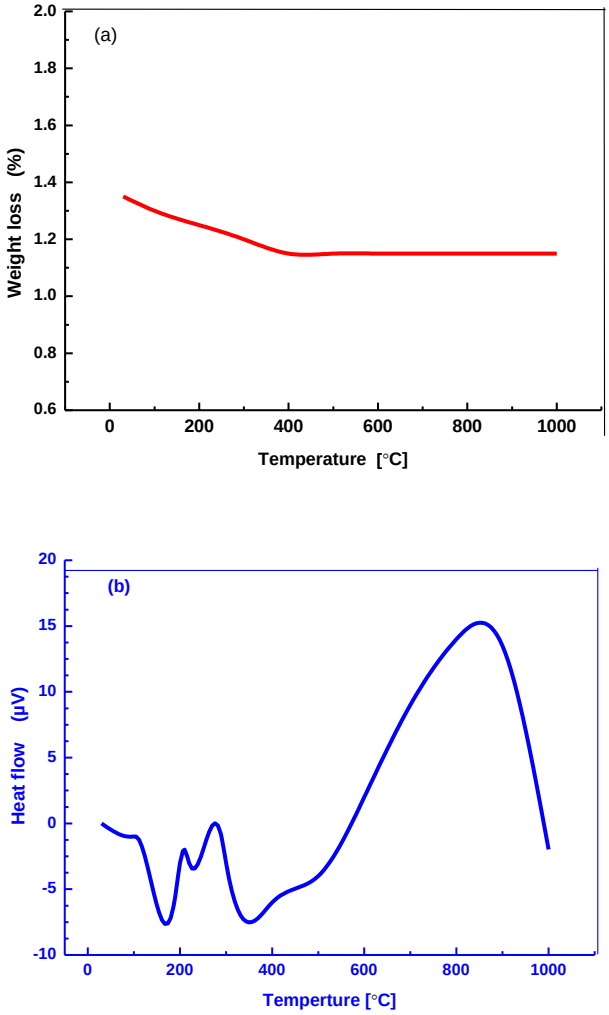

Fig. 3: Thermal analyses (a) TG and (b) DTA for non-irradiated green V-Biotite sample .

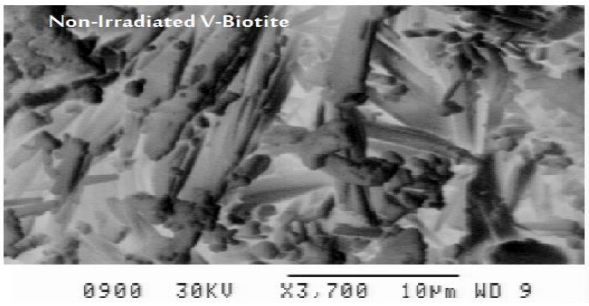

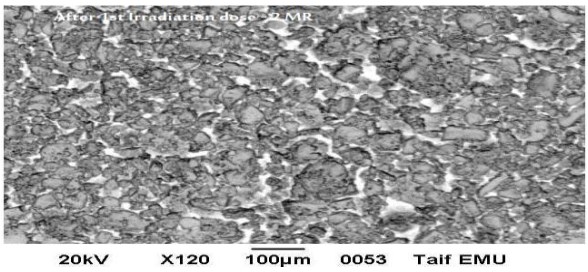

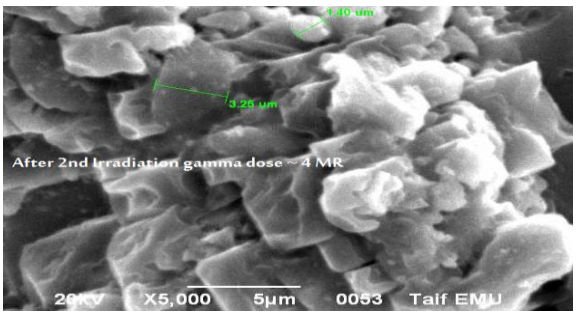

Fig. 4a-c: SEM photographs captured for V-Biotite sample before and after gamma irradiations .

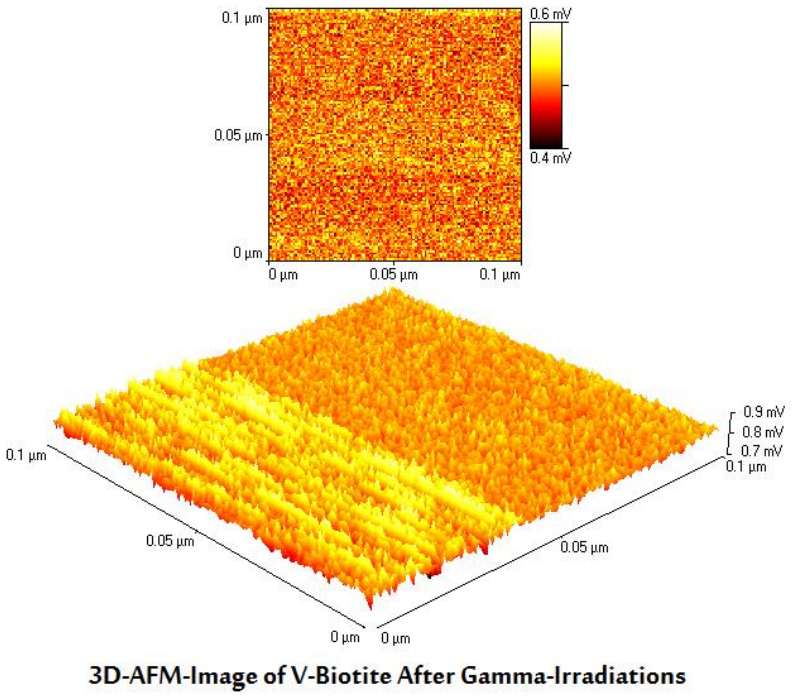

Fig.5: 2 & 3D-AFM image applying non-contact tapping mode for V-Biotite.

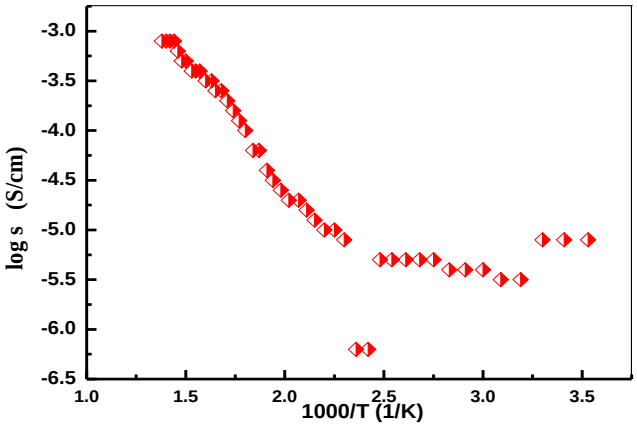

Fig. 6: Temperature dependence of the electrical conductivity of V-Biotite .

References:

[1] M.M.A.Sekkina,Khaled M.Elsabawy, High energy Nd-laser irradiation effect on optimally co-doped terbiumneodymium BPSCCO bismuth cuprate superconductor " *Physica C* 402 ,303-308,2004 .

[2] Khaled M.Elsabawy, W. F. Elhawary, Q. Mohsen and M.M.M.Youssef "Gamma-Irradiations Effects on Structural and Micro-Structural Parametersof Water Remediator HP- Mica- Cr-III-Clay Synthesized in Organic Solvent", *Materials Science J.* , Vol.5,4,pp. 382-386,2009 .

[3] Khaled M. Elsabawy, Morsy M. Abou-Sekkina, Gamma-Irradiations Effects on Structural and Micro-Structural Parameters of Chromium(III) – Silicate Base Mica Clay*J.of World Scientific News* -WSN 32, pp.26-36,2016.

[4] A. Zaykin and B. A. Aliyev, "Radiation effects in high-disperse metal media and their application in powder metallurgy," Radiation Physics and Chemistry, vol. 63, no. 3–6, pp. 227–230, 2002.

[5] F. Daniels, C. A. Boyd, and D. F. Saunders, Thermoluminescence as a research tool," Science, vol. 117, no. 3040, pp. 343–349, 1953.

[6] A. J. J. Bos, "High sensitivity thermoluminescence dosimetry," Nuclear Instruments and Methods in Physics Research B, vol. 184, pp. 3–28, 2001.

[7] R. P. Yavetskiy, E. F. Dolzhenkova, A. V. Tolmachev, S. V. Parkhomenko, V. N. Baumer, and A. L. Prosvirnin, "Radiation defects in $SrB_4O_7:Eu^{2+}$ crystals," Journal of Alloys and Compounds, vol. 441, no. 1-2, pp. 202–205, 2007.

[8] T. E. Schlesinger, J. E. Toney, H. Yoon et al., "Cadmium zinc telluride and its use as a nuclear radiation detector material," Materials Science and Engineering R, vol. 32, no. 4-5, pp. 103–189, 2001.

[9] W. L. McLaughlin, A. W. Boyed, K. C. Chadwich, J. C. Mcdonald, and A. Miller, Dosimetry for Radiation Processing, Taylor & Francis, London, UK, 1989.

[10] T. Nakajima and T. Otsuki, "Dosimetry for radiation emergencies: radiation-induced free radicals in sugar of various countries and the effect of pulverizing on the ESR signal," Applied Radiation and Isotopes, vol. 41, no. 4, pp. 359–365, 1990.

[11] T. Nakajima, "ESR of sugar as a personnel monitor for radiation emergencies," Applied Radiation and Isotopes, vol. 46, no. 8, pp. 819–825, 1995.

[12] A. Tchen, C. L. Greenstock, and A. Trivedi, "The use of sugar pellets in ESR dosimetry," Radiation Protection Dosimetry, vol. 46, no. 2, pp. 119–121, 1993.

[13] N. A. Atari and K. V. Ettinger, “Lyoluminescence of irradiated saccharides,” Radiation Effects, vol. 20, no. 1-2, pp. 135–139, 1973.

[14] T. Nickel, E. Pitt, and A. Scharmann, “Lyoluminescence dosimetry with a sugar after accidental gamma ray exposure,” Radiation Protection Dosimetry, vol. 35, no. 3, pp. 173–177, 1991.

[15] A. J. Walton, “Triboluminescence,” Advances in Physics, vol. 26, no. 6, pp. 887–948, 1977.

[16] G. Alzetta, I. Chudasek, and R. Scarmozzino, “Excitation of triboluminescence by deformation of single crystals,” Physica Status Solidi A, vol. 1, no. 4, pp. 775–785, 1970.

[17] Y. Enomoto and H. Hashimoto, “Emission of charged particles from indentation fracture of rocks,”Nature, vol. 346, no. 6285, pp. 641–643, 1990.

[18] T. Matsuzawa, Y. Aokiy, N. Takeuchi, and Y. Murayama, “A new long phosphorescent phosphor with high brightness, $SrAl_2O_4$: Eu^{2+}, Dy^{3+},” Journal of the Electrochemical Society, vol. 143, pp. 2670–2673, 1996.

[19] R. Dekkers and C. F. Woensdregt, “Crystal structural control on surface topology and crystal morphology of normal spinel (MgA_{l2O4}),” Journal of Crystal Growth, vol. 236, no. 1–3, pp. 441–454, 2002.

[20] C. Baud ń, R. Mart ńez, and P. Pena, “High-temperature mechanical behavior of stoichiometric magnesium spinel,” Journal of the American Ceramic Society, vol. 78, pp. 1857–1862,1995.

[21] M. Sindel, N. A. Travitzky, and N. Claussen, “Influence of magnesium-aluminum spinel on the directed oxidation of molten aluminum alloys,” Journal of the American Ceramic Society, vol. 73, pp. 2615–2618, 1990.

[22] Khaled M.Elsabawy, Part-II 3D-AFM-Microstructural Featues and Suitability of Sulfonyl-Urea Moeity as Center of Antidiabetic Drugs Families, , *Inter. Journal of Pharmaceutical Sci. (IJPMS) 1, Issue 1,* pp. 1-6,2015.

[23] Khaled M. Elsabawy Micro-Structural Features Suitability of Gramicidin Drug as Antibacterial Ointment Antibiotic *Int.J. Pharm. Toxicology,5,1,*pp.62-66,2015.

[24] Khaled M. Elsabawy, Impact of Double Irradiations on the Structural and Micro-structural Features of some Selected Solid Phase -Milk Products „; *Britsh Journal of Research,* 1,3 ,pp.124-133,2014.

[25] Khaled M. Elsabawy ,Spotlight on Nano-Structural Features of Solid-Phase Moxifloxacin Antibiotic An AFM-Investigations ,Khaled M. Elsabawy and Waheed F.El-Hawary,*Int.J.of Phytopharmacology*,5,4,pp.284-287,2014.